SCIENTIFIC REPORTS

OPEN

Field-free Magnetization Switching by Utilizing the Spin Hall Effect and Interlayer Exchange Coupling of Iridium

Received: 21 September 2018
Accepted: 10 December 2018
Published online: 23 January 2019

Yang Liu[1,3], Bing Zhou[1,3] & Jian-Gang (Jimmy) Zhu[2,3]

Magnetization switching by spin-orbit torque (SOT) via spin Hall effect represents as a competitive alternative to that by spin-transfer torque (STT) used for magnetoresistive random access memory (MRAM), as it doesn't require high-density current to go through the tunnel junction. For perpendicular MRAM, however, SOT driven switching of the free layer requires an external in-plane field, which poses limitation for viability in practical applications. Here we demonstrate field-free magnetization switching of a perpendicular magnet by utilizing an Iridium (Ir) layer. The Ir layer not only provides SOTs via spin Hall effect, but also induce interlayer exchange coupling with an in-plane magnetic layer that eliminates the need for the external field. Such dual functions of the Ir layer allows future build-up of magnetoresistive stacks for memory and logic applications. Experimental observations show that the SOT driven field-free magnetization reversal is characterized as domain nucleation and expansion. Micromagnetic modeling is carried out to provide in-depth understanding of the perpendicular magnetization reversal process in the presence of an in-plane exchange coupling field.

Research efforts in discovering and gaining better understanding of various spin-based physical phenomena over the past decades have propelled the innovation and developments of new generations of memory and logic devices[1–4]. With utilization of non-volatility inherent in magnetism and low-power consumption characteristics, these novel device concepts present new opportunities for future electronics and computers. One of the most renowned examples is the spin-transfer torque magnetoresistive random access memory (STT-MRAM)[5–8]. In STT-MRAM, spin polarized current can be generated and used to switch the magnetization direction via spin momentum transfer. In recent years, a three-terminal scheme for MRAM applications has been proposed that utilizes spin-orbit torques (SOTs) to switch the free layer[9–11]. Such scheme shows the benefits in lower current density as well as separate read- and write-path, and thus has attracted people's strong interests. In these devices, spin Hall effect (SHE)[12,13] is adopted as the main source for SOT injection[14–16]. It has been demonstrated that SHE can trigger magnetization switching of in-plane magnetic tunnel junctions (MTJs)[15,17,18]. For perpendicular MTJs that are required for high-density memory, an in-plane magnetic field has to be applied for SHE induced switching[16,18]. However, the need for an external applied field significantly hinders the technological viability of commercial applications.

By far, people have come up with several ways to solve this problem. One approach is by creating geometric asymmetry so that the SOTs acting on the perpendicular magnet could contain perpendicular components[19–21]. But this approach suffers the scalability issue. Another way is through introducing a local in-plane field via exchange bias or interlayer exchange coupling. It has been reported that an antiferromagnetic layer, such as PtMn[22] and IrMn[23,24], is able to generate spin current as well as add a horizontal field to the neighboring perpendicular magnetized layer by exchange bias so as to assist the switching. The detailed mechanisms, however, is not fully understood including SHE of antiferromagnetic materials as well as the large slopes in the switching loops. Moreover, YC Lau *et al.* obtained field-free magnetization reversal by using the interlayer exchange coupling via Ru[25]. But one limitation of this approach is that one cannot further add magnetoresistive layers to the film stack

[1]Department of Materials Science and Engineering, Carnegie Mellon University, Pittsburgh, Pennsylvania, 15213, USA. [2]Department of Electrical and Computer Engineering, Carnegie Mellon University, Pittsburgh, Pennsylvania, 15213, USA. [3]Data Storage Systems Center, Carnegie Mellon University, Pittsburgh, Pennsylvania, 15213, USA. Correspondence and requests for materials should be addressed to J.-G.(.Z. (email: jzhu@cmu.edu)

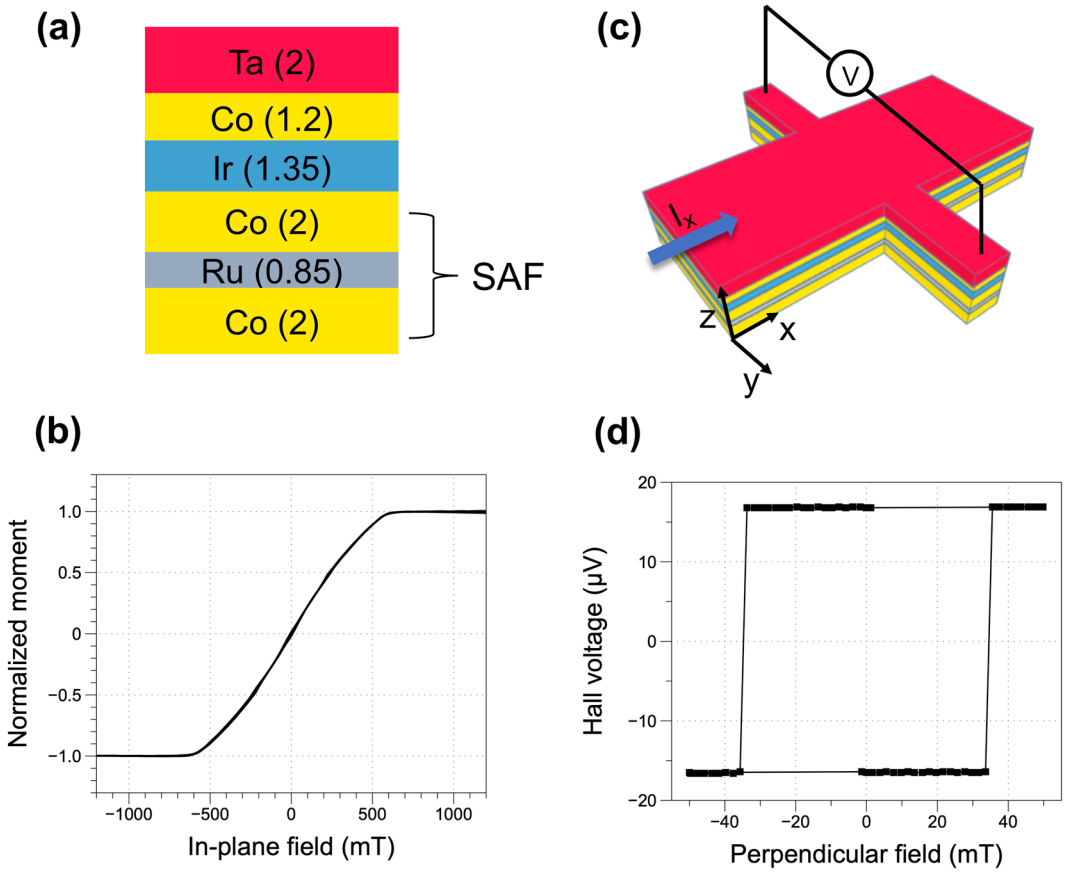

Figure 1. (**a**) Film stack for field-free magnetization switching, with unit in nanometers. (**b**) In-plane hysteresis loop of a pure SAF structure with the film stack of substrate/Ta/Co(2 nm)/Ru(0.85 nm)/Co(2 nm)/Ta. (**c**) Schematic illustration of the Hall-bar device for spin-orbit torque measurement. (**d**) Perpendicular-field-driven anomalous Hall effect loop for the device with the film stack shown in (**a**).

because the exchange coupling layer and spin Hall layer are separated. Although the scenario of using a Pt spacer was also demonstrated, the mechanism behind its interlayer exchange coupling still remains unclear.

Here, we demonstrate the realization of field-free magnetization switching by utilizing an Ir interlayer layer. Ir has been shown capable of generating spin Hall effect[26,27], and equally important for this study, it provides interlayer exchange coupling when sandwiched by two ferromagnetic layers, e.g. Co[28,29] at adequate thicknesses. Combing these two properties, we are able to achieve deterministic magnetization switching without an external in-plane field. We also investigate the switching process in our devices and characterize it as domain nucleation followed with SHE-induced domain wall motion (DWM).

Results

Magnetic properties. The film stack for field-free magnetization switching is substrate/Co(2)/Ru(0.85)/Co(2)/Ir(1.35)/Co(1.2)/Ta(2), with unit in nanometers. Here, the top thin Co layer is naturally perpendicularly magnetized due to the interfacial perpendicular anisotropy arising from the interface with the Ir layer[28,29]. The thickness of the Ir layer corresponds to the second antiferromagnetic coupling peak in the Ruderman–Kittel–Kasuya–Yosida (RKKY) thickness dependence curve (see supplementary information Fig. S1). The Co/Ru/Co below the Ir layer is a flux-matched in-plane synthetic antiferromagnetic (SAF) structure. The purpose of adopting the SAF instead of a single in-plane magnetized layer is to minimize the effect of the stray field on the perpendicular Co layer. The in-plane hysteresis loop of a fabricated SAF structure (Fig. 1(b)) shows strong interlayer exchange coupling and the loop shape indicates the single domain characteristics of the in-plane Co layers.

The film shown in Fig. 1(a) is patterned into Hall-cross devices with 4-μm wide current channel and 1-μm wide voltage channel. Figure 1(d) shows the measured Hall voltage arising from anomalous Hall effect (AHE) with varying external perpendicular fields. The squared shape of the AHE loop indicates well defined perpendicular magnetic anisotropy of the top Co layer.

SOT-driven magnetization switching. To study the SOT-driven magnetization switching, current pulses are injected along the current channel with each pulse length of 100 μs. The Hall voltage was measured after each write pulse with a read current of 100 μA, less than 1/10 of the writing current. Figure 2(a) shows the anomalous Hall voltage as a function of current density with a series of external fields, H_x, applied along the current direction. For $H_x > 20$ mT, well defined switching loops are obtained with positive and negative saturation values

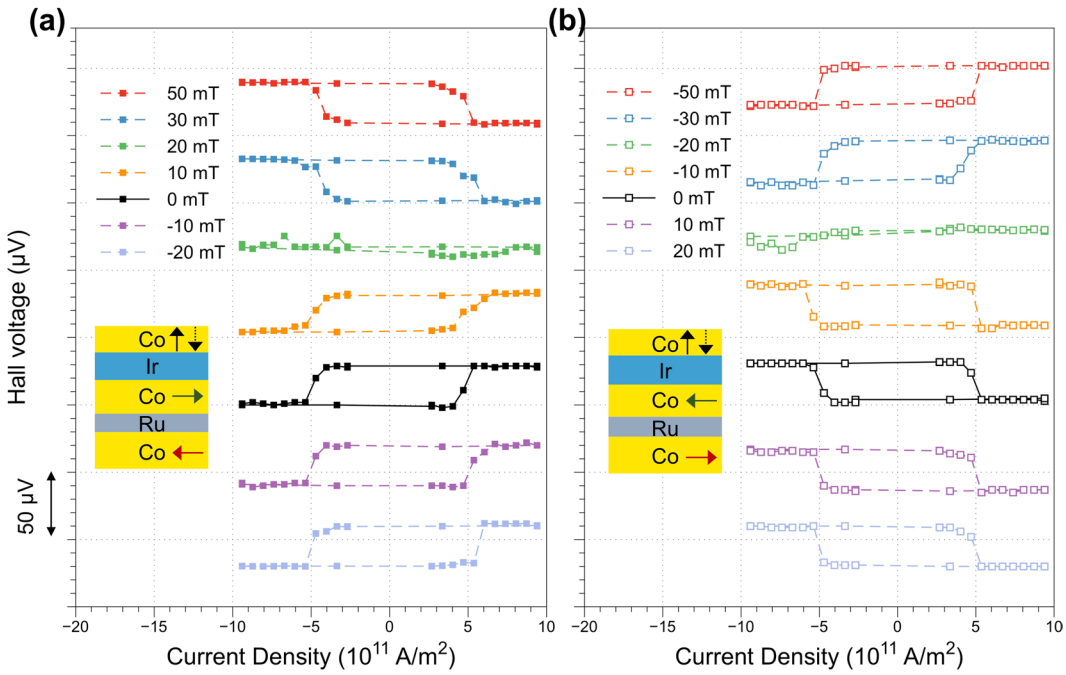

Figure 2. Anomalous Hall voltage as a function of injected current density in the Ir layer with various external magnetic fields H_x along the current direction. Bottom SAF is set as (**a**) ⇄, and (**b**) ⇆.

corresponding to the two perpendicular magnetization states. At $H_x = 20$ mT, the switching hysteresis loop collapses, indicating no magnetization switching occurs. At zero external field, the switching completely recovers, however, with flipped loop shape. The same switching loops are maintained for $H_x < 0$. Figure 2(b) shows the similar measurement sequence with the reversed magnetization of the bottom SAF structure (from ⇄ to ⇆). In contrast to that shown in Fig. 2(a), the collapse of the switching hysteresis loop now occurs at $H_x = -20$ mT instead.

It is our interpretation that when charge current flows into the Ir layer, pure spin current is generated due to spin Hall effect and then injected to the top perpendicular Co layer. This pure spin current drives the observed magnetization reversals provided there exists an in-plane magnetic field. At zero applied field, this in-plane field arises from the interlayer coupling between the perpendicular Co and in-plane Co layers above and below the Ir interlayer via the RKKY interaction. When the externally applied field cancels the coupling field in magnitude and direction exactly, magnetization reversal no longer occurs. Our evidence suggests this in-plane coupling field has a magnitude of 20 mT. It should be noted that the 20 mT coupling field shown in the devices is significantly smaller than that measured at film level, which is around 95 mT.

The above argument is further confirmed by the measurements on the devices that have the film stack without in-plane Co layer below Ir (see Supplementary information Fig. S2). AHE hysteresis loops resulting from perpendicular magnetization switching can only be obtained with external in-plane field whereas no current-induced switching is observed at zero field.

Switching process. To understand the nature of current-induced magnetization switching in the presence of the in-plane coupling field in our devices, Kerr microscopy is utilized to visualize magnetization reversal process, as shown in Fig. 3, with current pulses of 100 ns in duration. It's observed that small opposite domains nucleate at the beginning of the reversal. We notice the nucleation sites mostly locate around the device edge, where the perpendicular anisotropy should be lower than other device areas due to the damages caused by the etching process during device fabrication. Continued application of subsequent current pulses results in the expansion of the reversed domains in all directions. With sufficient number of current pulses, the region along the current pulses can be mostly reversed. We should note that there are always some small residual domains located sparsely along the current path that are difficult to eliminate, even with perpendicular magnetic field.

It's widely observed that SHE can induce domain wall motion (DWM) in heavy metal/ferromagnet systems[30–34]. One of the keys to the SHE-driven DWM is the Dzyaloshinskii-Moriya interaction (DMI) at heavy metal/ferromagnet that not only makes Neel-type domain walls more energetically favorable than Bloch-type ones but also introduces chirality to the domain wall structure[35–37]. Normally, up-down and down-up domain walls of an opposite domain possess the same chirality (either left- or right-handed), as shown in Fig. 3(b). These domain walls move in the same direction when receiving the SOTs from the neighboring heavy metal layer and thus domains can only shift forwards or backwards. With applying external in-plane field that's larger than the effective DMI field, up-down and down-up domain walls can have different chiral structures. As a result, a domain can either expand or shrink depending on the direction of injected current[38], which further leads to deterministic magnetization switching. In our case, we measured the effective DMI field at Ir/Co interface to be

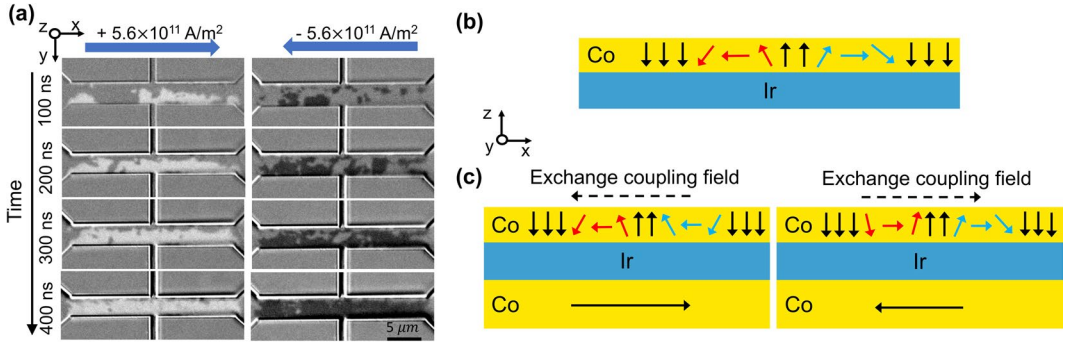

Figure 3. (**a**) Kerr microscope images showing the domain wall propagation during the current-induced magnetization switching process, without external magnetic field. Current is applied in +x (left) and −x (right) directions. Bottom SAF is set as ⇄. Between images in each column: 100-ns pulse, 1 pulse. (**b**) Schematic illustration of right-handed domain wall structures in Ir/Co system. Red arrows: down-up domain wall. Blue arrows: up-down domain wall. (**c**) Domain wall structures in presence of the exchange coupling field.

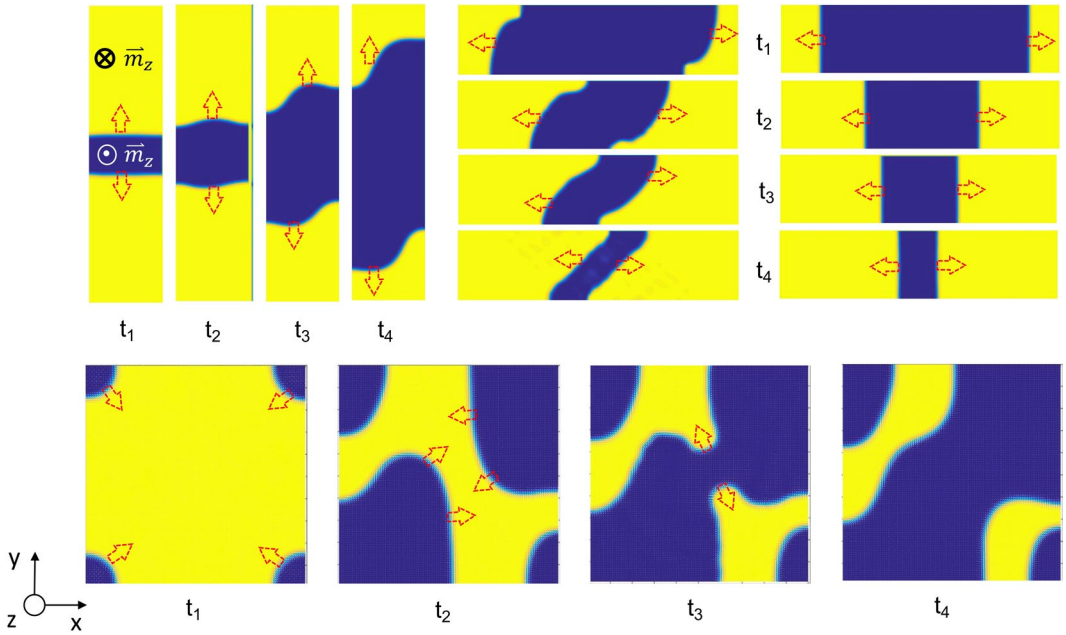

Figure 4. Simulated domain expansion in the perpendicular Co layer in the presence of the in-plane coupling field. The charge current flows along the +x direction. $t_1 < t_2 < t_3 < t_4$ represents the time evolution during the application of current.

about 9 mT (see supplementary information Fig. S4). Hence, the exchange coupling field (20 mT) in our devices is able to overcome the effective DMI field and give rise to the domain walls with opposite chirality (Fig. 3(c)). Based on our observations, it's the two types of domain walls moving in opposite directions that enables field-free magnetization switching. Therefore, the magnetization switching process in our devices can be interpreted as domain nucleation followed with SHE-driven DWM till the expansion of reversed domains produces full reversal.

Micromagnetic simulation. To provide further understanding of the experimental observations, the effect of pure spin current in the perpendicular Co layer is modeled by Slonczewski spin transfer torque included Landau-Lifshitz-Gilbert damped gyromagnetic equation of motion. The full stack is modeled with the bottom SAF structure set as ⇄. The modeling is carried out by initially creating a reversed domain, or domains, in a perpendicularly saturated top Co layer. Figure 4 shows sets of time evolution of domain configurations during the expansion of the initial reverse domains under the pure spin current. It is found that the reversed domains expand in all directions. Domain walls that are parallel to the interlayer exchange coupling field (as in the top left) move as fast as those orthogonal to the field (top right). It is interesting to note that as the reverse domains expand, the wall fronts often become curved during their motion (except when the wall front is perpendicular to the exchange field, as the case of top right in the Fig. 4 shows). This is because the wall moving speed is correlated with the orientation of magnetization component at the center of the wall. Figure 5 shows the wall speed as a function of the along-wall projection

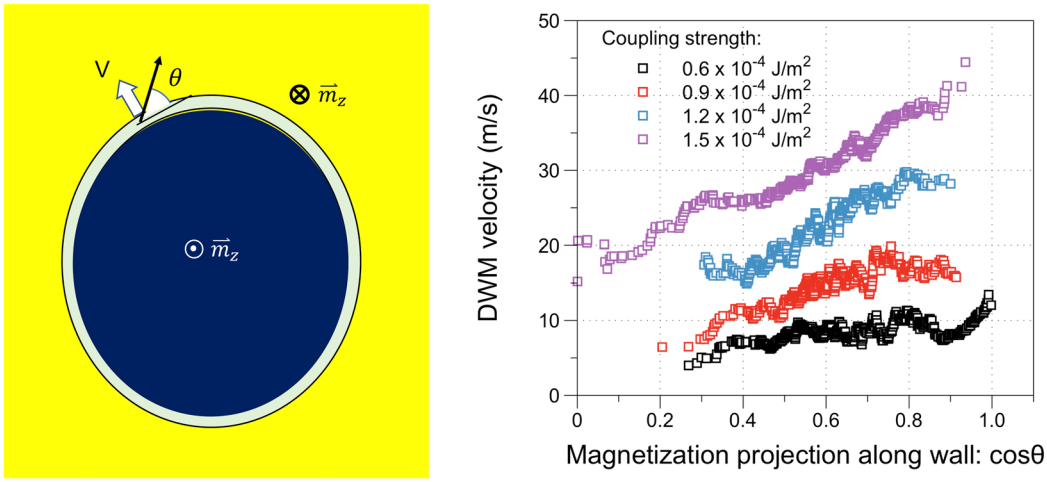

Figure 5. Calculated domain wall moving speed under the SHE generated spin current as a function of the direction cosine of the wall center magnetization along the wall tangent with four different in-plane coupling field strengths.

of the magnetization at the center of the wall with various interlayer exchange coupling strength. The simulation results suggest that the wall moves faster when the magnetization at the center of the wall becomes more parallel to the tangent of the wall. Furthermore, it can also be seen that not only the speed of DWM but also the slope of the speed angular dependence increase with higher interlayer exchange coupling field.

Discussion

Recently, CB Seung-heon, *et al.*[39] reported that spin current generated by the interface of non-magnetic metal/in-plane magnetized ferromagnet can contain some perpendicular polarization. Such perpendicular component of the spin current further gives rise to the SOTs that can achieve field-free magnetization switching. This mechanism can't be applied to explain our observations since the spin diffusion length of Ir is only 0.5 nm[40]. Therefore, even if such spin current is generated at Ir/in-plane Co interface it can't travel through the 1.35 nm-thick Ir layer to reach the top perpendicular Co layer.

Conclusion

To summarize, we achieved robust field-free magnetization switching by utilizing the SHE and interlayer exchange coupling of Ir. The switching process is dominated by SHE-induced domain wall propagation to achieve the full expansion of reserved domains. Combined modeling study shows that in the presence of the in-plane coupling field, the nucleated domains can expand in all directions and the higher the coupling field, the higher the expansion speed of the reversed domains. The domain wall speed also increases when the magnetization at the center of the wall becomes more parallel to the wall during the motion. It's noteworthy that the film stack we used is easy to be built up with magnetoresistive layers on the top. Meanwhile, the device size should be able to scale down to the dimension of tens of nanometers, which shows its potential for practical applications in memory and logic.

Methods

All films are deposited at room temperature by magnetron sputtering with base pressure $<2 \times 10^{-8}$ Torr. Film-level hysteresis loops are measured by Alternating Gradient Field Magnetometer (AGFM). The films are patterned into Hall-cross devices with 4-μ m wide current channel and 1-μm wide voltage channel utilizing e-beam lithography, optical lithography and ion beam etching. To study the SOT-driven magnetization switching, current pulses are injected along the current channel with each pulse length of 100 μs. The amplitude of the current at milliamp (mA) level is swept from negative to positive values and back to negative again. The Hall voltage was measured after each write pulse with a read current of 100 μA. Prior to writing, the moments of bottom SAF is initially set as ⇄ (or ⇆) by applying 1 T magnetic field in + x (or −x) direction. The current density is calculated with taking into the account both the resistivity and cross-section area of each layer. For studying the domain wall propagation during magnetization switching process, 100 ns current pulses are injected and the dynamics of magnetization reversal was tracked by Kerr microscope.

For DW modeling in our devices, the interlayer exchange coupling strength between the perpendicular Co layer and the in-plane Co layer sandwiching the Ir layer is varied throughout the study. The top perpendicular Co layer is assumed to have 2 nm thickness with interfacial perpendicular uniaxial anisotropy of $K_s = 4 \times 10^{-3}$ J/m^2 and saturation magnetization $M_s = 1.2$ T. The two Co layers in the Co/Ru/Co SAF are assumed to be flux-matched without perpendicular anisotropy and to have antiparallel exchange coupling of $\sigma_{ex,SAF} = -1.0 \times 10^{-3}$ J/m^2. The film stack is meshed laterally with each mesh cell of 2×2 nm^2 size. The exchange stiffness constant $A = 1.6 \times 10^{-11}$ J/m is assumed for all three Co layers. A spatially uniform pure spin current with spin polarization along the positive y-direction is assumed corresponding to a charge current density of $J_c = 10^{12}$ A/m^2 and a spin Hall angle of 10%. The top Co layer of the SAF is always magnetized along the positive x-direction with essentially uniform magnetization. Zero DMI is assumed for simplification.

Data Availability

All data gathered and/or analyzed in this study are included in the main article as well as the Supplementary Information.

References

1. Wolf, S. A. *et al*. Spintronics: a spin-based electronics vision for the future. *Science* **294**, 1488–95 (2001).
2. Žutić, I., Fabian, J. & Sarma, S. Das. Spintronics: Fundamentals and applications. *Rev. Mod. Phys.* **76**, 323–410 (2004).
3. Kent, A. D. & Worledge, D. C. A new spin on magnetic memories. *Nat. Nanotechnol.* **10**, 187–191 (2015).
4. Bromberg, D. M. *et al*. Experimental demonstration of four-terminal magnetic logic device with separate read- and write-paths. *Electron device Meet*. 792–795, https://doi.org/10.1109/IEDM.2014.7047159 (2014).
5. Huai, Y. Spin-transfer torque MRAM (STT-MRAM): Challenges and prospects. *AAPPS Bull.* **18**, 33–40 (2008).
6. Kishi, T. *et al*. Lower-current and fast switching of a perpendicular TMR for high speed and high density spin-transfer-torque MRAM. in *Electron Devices Meeting, 2008. IEDM 2008. IEEE International* 1–4 (IEEE, 2008).
7. Chen, E. *et al*. Advances and future prospects of spin-transfer torque random access memory. *IEEE Trans. Magn.* **46**, 1873–1878 (2010).
8. Diao, Z. *et al*. Spin-transfer torque switching in magnetic tunnel junctions and spin-transfer torque random access memory. *J. Phys. Condens. Matter* **19**, 165209 (2007).
9. Cubukcu, M., Boulle, O., Mikuszeit, N. & Hamelin, C. Ultra-fast magnetization reversal of a three-terminal perpendicular magnetic tunnel junction by spin-orbit torque. *Spintec* 1–23 1509.02375v1 (2015).
10. Jabeur, K., Di Pendina, G., Bernard-Granger, F. & Prenat, G. Spin orbit torque non-volatile flip-flop for high speed and low energy applications. *IEEE electron device Lett.* **35**, 408–410 (2014).
11. Prenat, G., Jabeur, K., Di Pendina, G., Boulle, O. & Gaudin, G. Beyond STT-MRAM, spin orbit torque RAM SOT-MRAM for high speed and high reliability applications. In *Spintronics-based Computing* 145–157 (Springer, 2015).
12. Hirsch, J. E. Spin hall effect. *Phys. Rev. Lett.* **83**, 1834 (1999).
13. Dyakonov, M. I. & Khaetskii, A. V. Spin hall effect. In *Spin physics in semiconductors* 211–243 (Springer, 2008).
14. Van den Brink, A. *et al*. Spin-Hall-assisted magnetic random access memory. *Appl. Phys. Lett.* **104**, 12403 (2014).
15. Liu, L. Spin-torque switching with the giant spin Hall effect of tantalum. *Science (80-.).* **336**, 555–558 (2012).
16. Liu, L., Lee, O. J., Gudmundsen, T. J., Ralph, D. C. & Buhrman, R. A. Current-induced switching of perpendicularly magnetized magnetic layers using spin torque from the spin Hall effect. *Phys. Rev. Lett.* **109**, 96602 (2012).
17. Pai, C. F. *et al*. Spin transfer torque devices utilizing the giant spin Hall effect of tungsten. *Appl. Phys. Lett.* **101**, 1–5 (2012).
18. Fukami, S., Anekawa, T., Zhang, C. & Ohno, H. A spin–orbit torque switching scheme with collinear magnetic easy axis and current configuration. *Nat. Nanotechnol.* 1–6, https://doi.org/10.1038/nnano.2016.29 (2016).
19. Yu, G. *et al*. spin – orbit torques in the absence of external magnetic fields. **9** (2014).
20. You, L. *et al*. Switching of perpendicularly polarized nanomagnets with spin orbit torque without an external magnetic field by engineering a tilted anisotropy. *Proc. Natl. Acad. Sci.* **112**, 10310–10315 (2015).
21. Kazemi, M., Rowlands, G. E., Shi, S., Buhrman, R. A. & Friedman, E. G. All-spin-orbit switching of perpendicular magnetization. *IEEE Trans. Electron Devices* **63**, 4499–4505 (2016).
22. Fukami, S., Zhang, C., DuttaGupta, S., Kurenkov, A. & Ohno, H. Magnetization switching by spin–orbit torque in an antiferromagnet–ferromagnet bilayer system. *Nat. Mater.* **15**, 535 (2016).
23. van den Brink, A. *et al*. Field-free magnetization reversal by spin-Hall effect and exchange bias. *Nat. Commun.* **7**, 10854 (2016).
24. Oh, Y.-W. *et al*. Field-free switching of perpendicular magnetization through spin–orbit torque in antiferromagnet/ferromagnet/oxide structures. *Nat. Nanotechnol.* **11**, 878 (2016).
25. Lau, Y.-C., Betto, D., Rode, K., Coey, J. M. D. & Stamenov, P. Spin–orbit torque switching without an external field using interlayer exchange coupling. *Nat. Nanotechnol.* **11**, nnano–2016 (2016).
26. Zhang, W. *et al*. Spin pumping and inverse spin Hall effects — Insights for future spin-orbitronics (invited) **180901**, 1–7 (2016).
27. Niimi, Y. *et al*. Extrinsic spin Hall effect induced by iridium impurities in copper. *Phys. Rev. Lett.* **106**, 126601 (2011).
28. Yakushiji, K., Sugihara, A., Fukushima, A., Kubota, H. & Yuasa, S. Very strong antiferromagnetic interlayer exchange coupling with iridium spacer layer for perpendicular magnetic tunnel junctions. *Appl. Phys. Lett.* **110**, 92406 (2017).
29. Huai, Y. *et al*. High performance perpendicular magnetic tunnel junction with Co/Ir interfacial anisotropy for embedded and standalone STT-MRAM applications. *Appl. Phys. Lett.* **112**, 92402 (2018).
30. Miron, I. M. *et al*. Fast current-induced domain-wall motion controlled by the Rashba effect. *Nat. Mater.* **10**, 419–423 (2011).
31. Haazen, P. P. J. *et al*. Domain wall depinning governed by the spin Hall effect. *Nat. Mater.* **12**, 299–303 (2013).
32. Parkin, S. & Yang, S.-H. Memory on the racetrack. *Nat. Nanotechnol.* **10**, 195–198 (2015).
33. Liu, Y., Furuta, M. & Zhu, J.-G. Spin Hall driven domain wall motion in magnetic bilayers coupled by a magnetic oxide interlayer. *AIP Adv.* **8**, 56306 (2018).
34. Liu, Y., Liu, X. & Zhu, J.-G. Tailoring the Current-Driven Domain Wall Motion by Varying the Relative Thickness of Two Heavy Metal Underlayers. *IEEE Trans. Magn* (2018).
35. Emori, S., Bauer, U., Ahn, S.-M., Martinez, E. & Beach, G. S. D. Current-driven dynamics of chiral ferromagnetic domain walls. *Nat. Mater.* **12**, 611–6 (2013).
36. Ryu, K.-S., Thomas, L., Yang, S.-H. & Parkin, S. S. P. Chiral spin torque at magnetic domain walls. *Nat. Nanotechnol.* **8**, 527–33 (2013).
37. Ryu, K.-S., Yang, S.-H., Thomas, L. & Parkin, S. S. P. Chiral spin torque arising from proximity-induced magnetization. *Nat. Commun.* **5**, 3910 (2014).
38. Lee, O. J. *et al*. Central role of domain wall depinning for perpendicular magnetization switching driven by spin torque from the spin Hall effect. *Phys. Rev. B - Condens. Matter Mater. Phys.* **89**, 1–8 (2014).
39. Seung-heon, C. B. *et al*. Spin currents and spin–orbit torques in ferromagnetic trilayers. *Nat. Mater.* **17**, 509 (2018).
40. Zhang, W. *et al*. Determination of the spin diffusion length via spin pumping and spin Hall effects. in *APS March Meeting Abstracts* (2014).

Acknowledgements

This work was funded by a Laboratory Directed Research and Development grant from Sandia National Laboratories. Sandia National Laboratories is a multi-mission laboratory managed and operated by National Technology and Engineering Solutions of Sandia, LLC., a wholly owned subsidiary of Honeywell International, Inc., for the U.S. Department of Energy's National Nuclear Security Administration under contract DE-NA0003525. The authors thank Calvin Chan and Alex Roesler for their support.

Author Contributions

Y.L., B.Z. and J.Z. contributed evenly on the idea of the study. Y.L. and B.Z. conducted experimental works including film deposition, device fabrication and measurements. J.Z. performed micromagnetic simulations. Y.L. and J.Z. wrote the manuscript.

Additional Information

Supplementary information accompanies this paper at https://doi.org/10.1038/s41598-018-37586-4.

Competing Interests: The authors declare no competing interests.

Publisher's note: Springer Nature remains neutral with regard to jurisdictional claims in published maps and institutional affiliations.